Available online at www.sciencedirect.com
SCIENCE DIRECT
ELSEVIER
International Journal of Mass Spectrometry 249–250 (2006) 451–461
International Journal of Mass Spectrometry
www.elsevier.com/locate/ijms

On the reaction of ground-state nitrogen atoms with bromomethyl radicals: A computational study

Alvaro Cimas [a,b], Víctor M. Rayón [a], Massimiliano Aschi [b,*], Carmen Barrientos [a], José A. Sordo [c], Antonio Largo [a,**]

[a] *Departamento de Química Física, Facultad de Ciencias, Universidad de Valladolid, 47005 Valladolid, Spain*
[b] *Dipartimento di Chimica, Ingegneria Chimica e Materiali, Universitá di L'Aquila, Via Vetoio (Coppito 2), I-67010 L'Aquila, Italy*
[c] *Laboratorio de Química Computacional, Departamento de Química Física y Analítica, Facultad de Química, Universidad de Oviedo, 33006 Oviedo, Spain*

Received 9 October 2005; received in revised form 9 November 2005; accepted 9 November 2005
Available online 20 December 2005

Dedicated to the memory of Prof. Chava Lifschitz.

Abstract

A computational study of the reaction of N(^{4}S) with CH_2Br radicals has been carried out. The reaction starts through the formation of a relatively stable intermediate which does not involve an energy barrier. The two most exothermic products are those resulting from the release of a bromine atom, $H_2C=N+Br$ and *trans*-$HC=NH+Br$. A kinetic study, within the framework of the statistical theories, shows that the most exothermic product, namely $H_2C=N+Br$, is also the preferred product under kinetic control, whereas only minor fractions of $HBrCN+H$ are predicted at all temperatures. Therefore, the mechanistic characteristics observed for the N(^{4}S) + CH_2Br reaction are very similar to the N(^{4}S) + CH_2Cl reaction, but quite different from those found in the case of N(^{4}S) + CH_2F, where the preferred channel corresponds to formation of HFCN through elimination of a hydrogen atom. The rate coefficient for the title reaction is estimated to be about 9×10^{-13} cm^3 s^{-1} molecule^{-1} at 300 K, showing that should proceed with a high efficiency.

Keywords: Gas-phase reaction; Radical reactivity; Chemical kinetics; Quantum chemistry

1. Introduction

The reactions of oxygen and nitrogen atoms with different halogenated alkyl radicals have recently been studied both experimentally [1–8] and theoretically [9–16]. The interest on these reactions is due to their relevance in atmospheric and combustion chemistry. In addition, these processes are radical–radical reactions, a type of reactions that are not only very important in atmospheric chemistry [17,18], but also of general relevance in gas-phase chemistry. Therefore, theoretical studies might be valuable for understanding the mechanisms involved in these processes.

Recently, two different theoretical studies have been conducted for the reactions of ground-state nitrogen atoms with CH_2F radicals [14,15], whereas another recent theoretical work [16] has addressed the study of the reaction of N(^{4}S) with chloromethyl radicals. One of the most interesting aspects of these studies is the effect of halogenation in the reactions of ground-state nitrogen with alkyl radicals. The reaction of N(^{4}S) with methyl radicals has been studied both experimentally [19,20] and theoretically [21,22], due to its relevance in astrophysics [23,24] and in combustion processes [25]. In the case of the reaction of ground-state nitrogen with methyl radicals, experimental studies [20] have shown that the preferred product is H_2CN+H. For the N(^{4}S) + CH_2F reaction theoretical studies predict [14,15] that the major product should be (branching ratio ≈0.75) $HFCN+H$, with H_2CN+F as secondary product (branching ratio ≈0.23). On the other hand, for the analogue reaction with chloromethyl radical the computational studies [16] predict that release of chlorine atoms, resulting in H_2CN+Cl, should be the most favored channel both from the thermodynamic and kinetic points of view, with an estimated branching ratio of nearly 0.97. Therefore, it seems that

* Corresponding author. Tel.: +39 0862 43 3775; fax: +39 0862 43 3753.
** Corresponding author.
E-mail addresses: aschi@caspur.it (M. Aschi), alargo@qf.uva.es (A. Largo).

1387-3806/$ – see front matter © 2005 Elsevier B.V. All rights reserved.
doi:10.1016/j.ijms.2005.11.008

there is a different behavior depending on the nature of the substituting halogen. In the case of the fluorinated radical elimination of a hydrogen atom is favored, whereas for CH_2Cl release of chlorine seems to be the dominant channel.

In the present work a theoretical study of the reaction of $N(^4S)$ with CH_2Br is carried out on the spin conserving surface. In this respect it may be important to point out that quintet surface does not show any thermochemically and kinetically relevant intermediate. As far as the occurrence of spin non-conserving processes is concerned, further calculations are currently in progress. A kinetic study within the frame of the statistical theories will be also presented. Furthermore, a comparison with the previous studies on the reactions of $N(^4S)$ with CH_2F and CH_2Cl will be made.

2. Computational methods

The theoretical methods employed in this work are similar to those used in our previous study of the $N(^4S) + CH_2F$ and $N(^4S) + CH_2Cl$ reactions [14–16]. Geometrical parameters and vibrational frequencies for the different species involved in the reaction of ground-state nitrogen atoms with bromomethyl radicals have been obtained employing two different theoretical methods, namely second-order Møller-Plesset (MP2) [26] and density functional (DFT) [27] theories. In both cases we employed Dunning's triple-zeta cc-pVTZ basis set [28]. In the case of DFT calculations we have chosen the so-called B3LYP level, which is a combination of Becke's three-parameter exchange functional [29] and the correlation functional of Lee–Yang–Parr [30]. In order to obtain more accurate energies we have also employed different approaches. In first place, we have carried out calculations at the MP2 and B3LYP levels with the cc-pVXZ (X = D, T, Q) correlated–consistent basis sets and performed extrapolations [31] to estimate complete basis set (CBS) limits. In particular, we used a mixed exponential/Gaussian function of the form

$$E_{CBS} = E(x) - B\exp[-(x-1)] - C\exp[-(x-1)^2] \qquad (1)$$

where x = 2 (DZ), 3 (TZ), or 4 (QZ), and B and C are fitting constants. Even though other expressions are also available, it seems that the different extrapolation models lead to similar results [32]. One potential problem when dealing with open-shell systems is the possibility of spin contamination, which might affect the convergence of the MP series. Therefore, in order to mitigate this problem, we employed approximate projected MP2 energies [33]. On the other hand, DFT calculations are virtually free of spin contamination.

In addition to extrapolated MP2 and B3LYP energies, we have also employed two different levels of theory in order to refine the electronic energy and to compare their performance. At the B3LYP geometries we carried out CCSD(T) calculations [34] (coupled cluster with single and double excitations model augmented with a non-iterative triple excitation correction) with the cc-pVTZ basis set. Furthermore, G2 [35] calculations, which employ MP2 geometries, were carried out. In this level of theory the electronic energy is computed (making additivity assumptions) at the QCISD(T)/6-311 + G(3df, 2p) level, where QCISD(T) stands for a quadratic configuration interaction with single and double excitations, followed by a perturbative treatment of triple excitations. The G2 calculations were performed according to the standard procedure [35], with the only exception of the use of projected-MP energies instead of unprojected ones.

All transition states were characterized according to their imaginary vibrational frequency. In addition, the intrinsic reaction coordinate (IRC) method [36,37] was employed to check that they connect the desired minima located on the potential energy surface (PES). All quantum chemical calculations were performed with the GAUSSIAN 98 package of programs [38].

In order to obtain more founded conclusions about the preferred channels for the title reaction, we have carried out kinetic calculations within the framework of the statistical kinetic theories. For the formation of the initial intermediate, as well as for those processes where no transition structure was found (i.e. direct dissociations), we have employed the microcanonical variational transition state theory (μVTST) in its vibrator formulation [39,40]. For this purpose we have made scans for all these paths. Subsequently, for each point of the scan, the Hessian matrices, describing the modes orthogonal to the reaction path, were evaluated according to the standard procedure of Miller [41,42].

For the unimolecular processes involving all the intermediates, the microcanonical rate coefficients have been calculated employing the usual Eq. (2) of RRKM theory [43].

$$k(E, J) = \sigma N^{\#}(E, J)/h\rho(E, J) \qquad (2)$$

where σ is the reaction symmetry factor, $N^{\#}(E, J)$ and $\rho(E, J)$ are, respectively, the number of states at the transition state and the density of states at the minimum evaluated for an energy E and a total angular momentum J.

The determination of the density and sum of states was carried out with the Forst algorithm [44] using the corresponding frequencies and moments of inertia (all required data for intermediates and transition states are provided in Tables S1 and S2 of the Supporting Information). The possibility of tunneling was accounted for in terms of a monodimensional probability according to the generalized Eckart potential [45]. Finally, thermal rate coefficients were evaluated by averaging over the Boltzmann distribution. All the kinetic calculations were carried out with our own routines, employing the CCSD(T)/cc-pVTZ//B3LYP/cc-pVTZ energies and B3LYP/cc-pVTZ geometries and vibrational frequencies, just as in our previous study on the $N(^4S) + CH_2Cl$ reaction [16].

3. Results and discussion

First, we will comment on the most interesting features of the triplet potential energy surface of the title reaction. We will focus on the most feasible reaction products from the thermodynamic viewpoint and discuss on the possible channels leading to such products. To get insights on the kinetics of this reaction, we have undergone a kinetic study within the framework of statistical

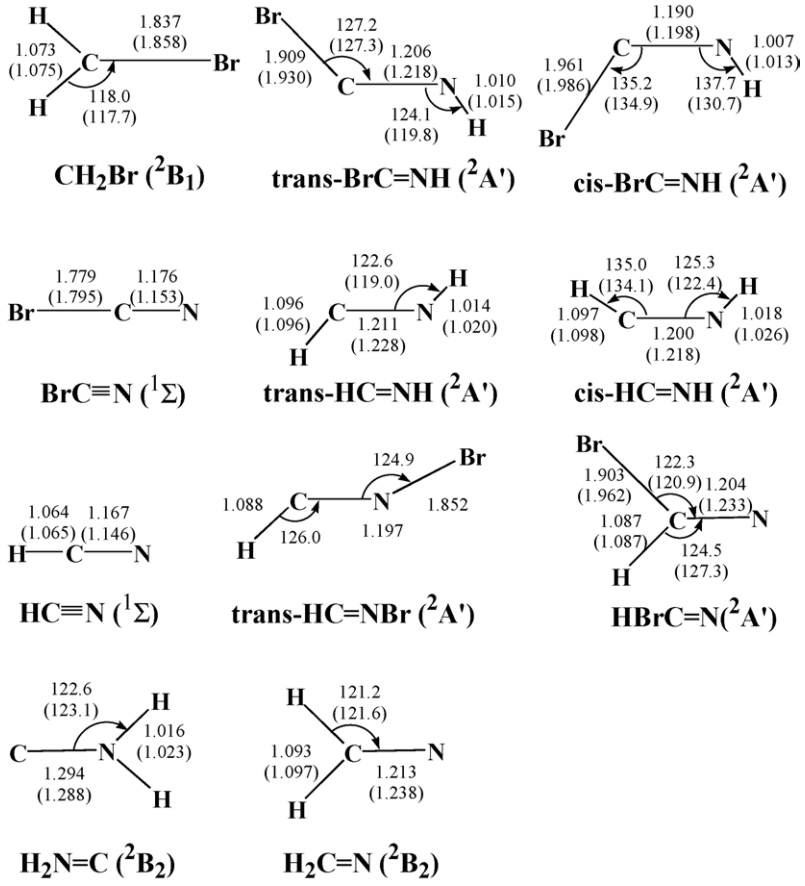

Fig. 1. Geometrical parameters as computed at the MP2/cc-pVTZ and B3LYP/cc-pVTZ (in parentheses) levels for the reactant and possible products of the reaction $N(^4S) + CH_2Br$. Bond distances are given in angstroms and angles in degrees.

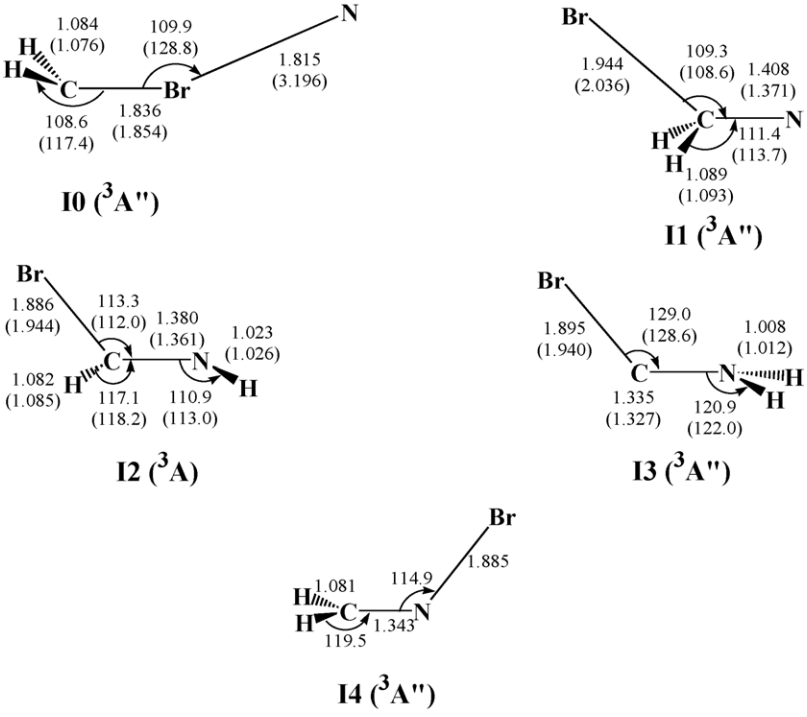

Fig. 2. Geometrical parameters as computed at the MP2/cc-pVTZ and B3LYP/cc-pVTZ (in parentheses) levels for the intermediates in the reaction of $N(^4S) + CH_2Br$. Bond distances are given in angstroms and angles in degrees.

theories. The most interesting results of the kinetic study will be commented in the second part of this work.

3.1. [NCH_2Br] triplet PES

Fig. 1 shows the most representative geometrical parameters for the reactant and possible products of the title reaction, whereas the geometries of intermediates and transition structures on the triplet surface are collected in Figs. 2 and 3, respectively. We have checked that intermediates have all their vibrational frequencies real and transition structures one imaginary frequency corresponding to the desired normal mode. Relative energies for the different species involved in the reaction have been collected in Table 1. Finally, Fig. 4 shows the energetic profile of the reaction up to formation of primary products and Fig. 5 shows the possible evolution of these primarily formed species by release of either bromine or hydrogen atoms.

Inspection of the data collected in Figs. 1–3 shows that MP2 and B3LYP methods yield in general very similar geometrical parameters. Nevertheless, some interesting discrepancies are encountered. For example, B3LYP agrees with experimental studies [46,47] which conclude that the reactant CH_2Br is planar, whereas MP2 predicts CH_2Br to be non-planar. However, both the small deviation from planarity of the MP2 C_s-symmetry minimun (the dihedral angle HCNH is 174.5°) and the low imaginary frequency of the transition vector in the planar transition structure (74i cm^{-1}), allow us to assume C_{2v} symmetry for this species whose electronic state is then $^2B_1$. We would also like to point out that neither products nor intermediates having a N–Br bond have been found on the B3LYP surface. The same result was also found in the [NCH_2Cl] triplet surface. This discrepancy between MP2 and B3LYP is not very important, because the product *trans*-HC=NBr lies relatively high in energy and, therefore, it is not one of the preferred products of the reaction (*cis*-HC=NBr has not been located in either the MP2 or B3LYP surfaces). The C–Br bond distance is relatively sensitive to the level of theory. For the reactant and products, this bond distance is predicted to be around 0.016–0.059 Å shorter at the MP2 level of theory. In the intermediates **I1**–**I3** this difference increases to 0.045–0.092 Å. The experimental C–Br bond distance in CH_2Br has been estimated recently [46] as r_0 = 1.848 Å which compares rather well to the computed values: r_e = 1.837 Å (MP2) and r_e = 1.858 Å (B3LYP). The C–N bond distances are predicted shorter at the MP2 level in some cases (maximun discrepancy: −0.037 Å in **I1**) but larger in some others (+0.029 Å in HBrC=N). Larger discrepancies are found in the geometries of the transition structures (see Fig. 3; according to recent theoretical studies [48], hybrid methods tend to predict looser transition structures). In any case, the geometrical differences are quantitative rather than qualitative. Except perhaps in the case of **TS1** (commented bellow) it seems clear that all the transition structures located on both surfaces represent the same transition states.

Table 1
Relative energies (in kcal mol^{-1}) at different levels of theory for the different species involved in the reaction of N(^{4}S) with CH_2Br ($^2B_1$)

System	PMP2/CBS[a]	G2[b]	B3LYP/CBS[c]	CCSD(T)[d]
$CH_2Br(^2B_1)$ + N(^{4}S)	0.0	0.0	0.0	0.0
trans-BrC•=NH + H•	−40.1	−34.4	−39.3	−27.4
cis-BrC•=NH + H•	−39.1	−32.7	−38.0	−25.6
BrC≡N + H• + H•	−18.9	−7.8	−4.4	−0.9
trans-HC•=NH + Br•	−55.5	−58.0	−68.3	−50.9
cis-HC•=NH + Br•	−51.1	−53.3	−64.5	−46.5
HC≡N + H• + Br•	−46.2	−42.3	−46.4	−35.2
trans-HC•=NBr + H•	−13.6	−11.2	–	–
HBrC=N• + H•	−39.6	−38.6	−41.3	−31.9
H_2C=N• + Br•	−60.3	−66.5	−76.3	−59.8
•C=$NH_2(^2B_2)$ + Br•	−32.4	−35.6	−46.1	−29.4
I0	+25.1	+20.9	−0.3	0.8
I1	−68.5	−68.9	−73.8	−63.3
I2	−58.8	−58.4	−65.5	−51.9
I3	−64.3	−60.3	−67.0	−53.7
I4	−49.1	−52.5	–	–
TS1	−61.7	−65.2	−72.6	−60.7
TS2	−32.7	−32.8	−38.4	−26.4
TS3	−26.9	−25.7	−31.5	−19.9
TS4	−26.4	−25.4	−31.2	−17.7
TS5	−32.6	−30.3	−37.8	−25.3
TS6	−51.9	−53.9	−61.7	−46.7
TS7	−20.9	−17.8	−24.2	−11.2
TS8	−27.2	−25.4	−33.3	−18.8
TS9	−37.2	−35.6	−38.3	−28.8
TS10	−40.8	−43.1	−54.7	−35.5
TS11	−30.8	−32.1	−41.3	−25.3
TS12	−34.0	−36.5	−42.8	−28.9
TS13	−5.2	−0.7	1.1	6.8
TS14	−8.8	−2.8	−6.2	5.0
TS15	−13.0	−7.7	−13.2	−0.8
TS16	−5.4	+0.3	−1.1	6.9
TS17	−20.9	−22.4	−30.5	−14.3

[a] Including ZPE at the MP2/cc-pVTZ level.
[b] Since no HF structure was found, the ZPE correction was carried out at the MP2(FULL)/6-31G(d) level (scaled by 0.96).
[c] Including ZPE at the B3LYP/cc-pVTZ level.
[d] Calculations CCSD(T)/cc-pVTZ//B3LYP/cc-pVTZ.

The data collected in Table 1 shows that the general trend in the relative energies is ΔH_0 (CCSD(T)/cc-pVTZ) < ΔH_0 (G2) ≈ ΔH_0 (MP2/CBS) < ΔH_0 (B3LYP/CBS). In previous studies on the N(^{4}S) + CH_2F/CH_2Cl reactions [14,16], we commented that the discrepancies between the CCSD(T) and G2 relative energies may be ascribed to two factors: in first place, the lack of the empiric high-level correction (HLC) in the CCSD(T) values, which seems to be important for a correct description of N(^{4}S), and, on the other hand, the cc-pVTZ basis set used in the CCSD(T) calculations which is still about 4 and 5 kcal mol^{-1} from the CBS limit (estimation done at the MP2 level). It seems to us that the same two factors also hold here and explain the differences of ∼7 kcal mol^{-1} between the CCSD(T) and G2 values.

A brief comment on S^2 expectation values is also in order. In Table S3 we provide the electronic energies at the G2 and CCSD(T)/cc-pVTZ levels, as well as the HF/cc-pVTZ S^2 expectation values for the different species involved in the reaction of N(^{4}S) with CH_2Br. As can be seen in Table S3, most species have $\langle S^2 \rangle$ values which exceed the spin-pure value by less than 10%. Nevertheless, we have checked the T1 diagnostic [49] to asses that single-reference based methods are reliable. In addi-

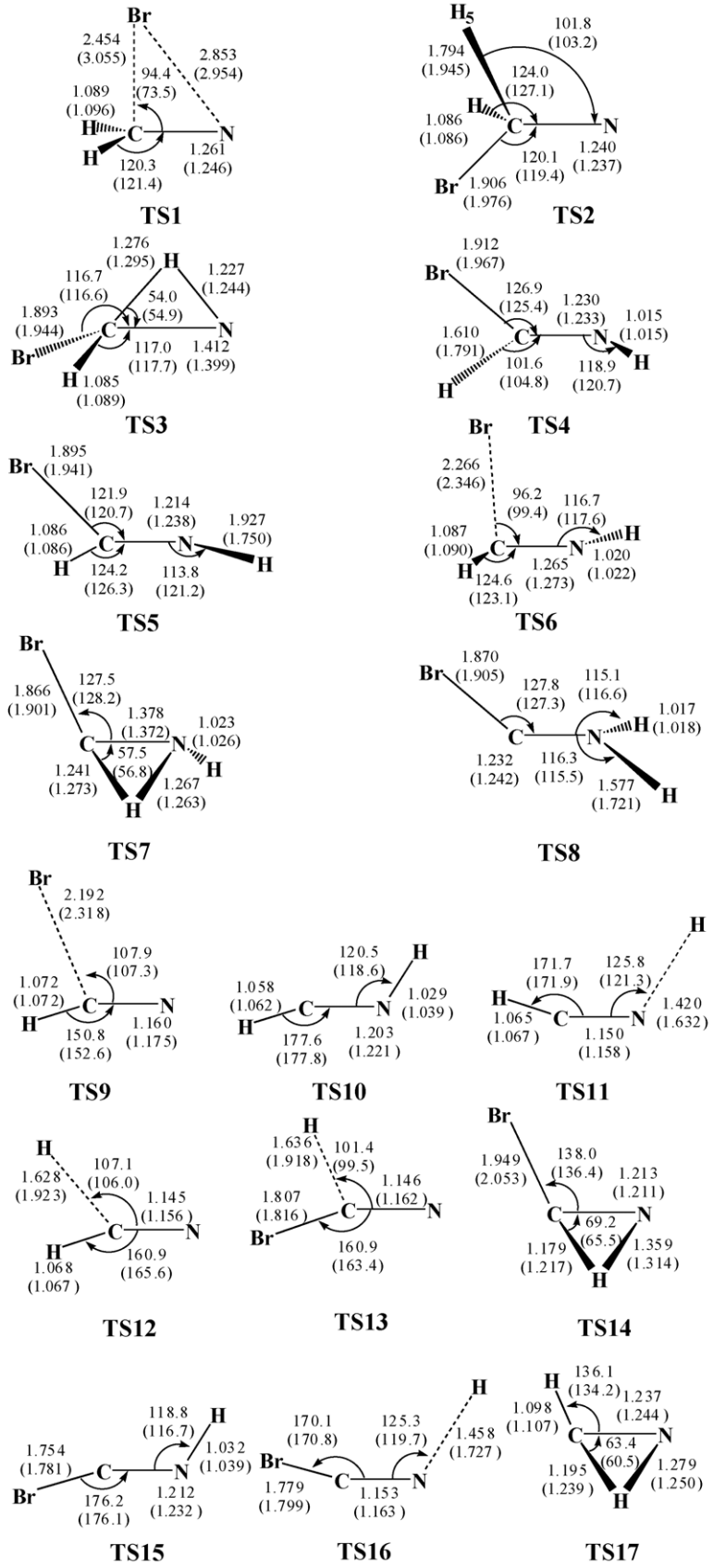

Fig. 3. Geometrical parameters as computed at the MP2/cc-pVTZ and B3LYP/cc-pVTZ (in parentheses) levels for the transition structures in the reaction of $N(^4S) + CH_2CBr$. Bond distances are given in angstroms and angles in degrees.

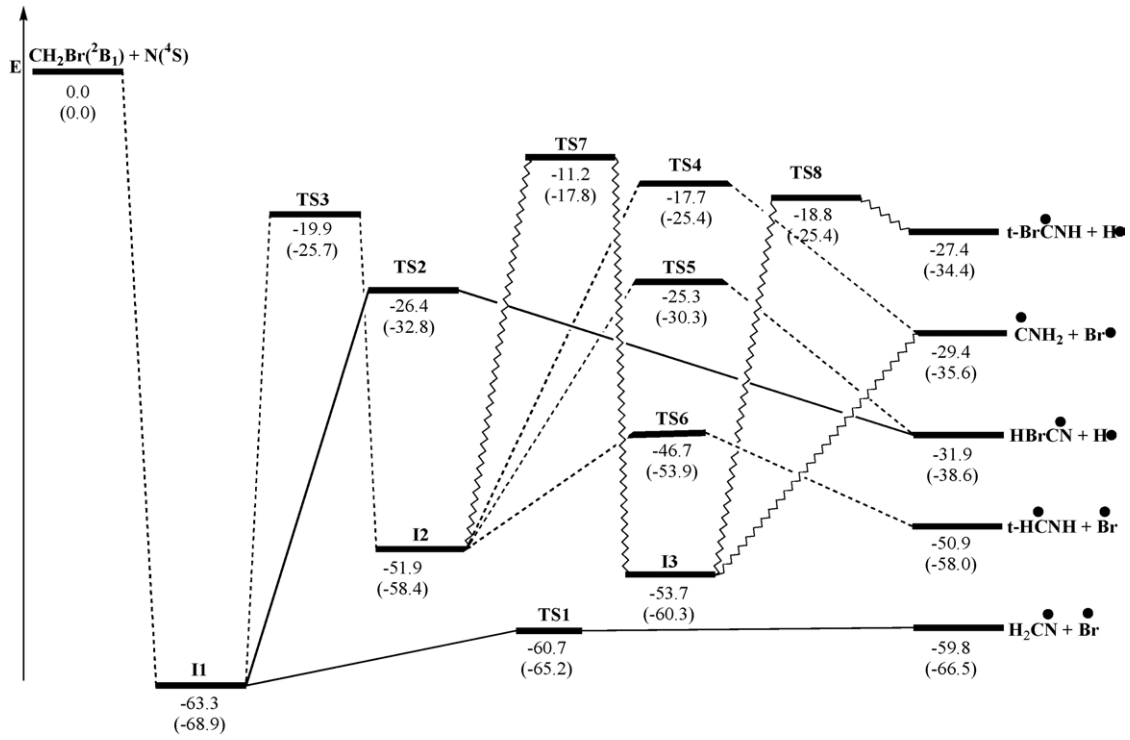

Fig. 4. Reaction profile (kcal mol^{-1}) at the CCSD(T)/cc-pVTZ and G2 (in parentheses) levels for the formation of the primary products resulting from elimination of either hydrogen or chlorine atoms in the reaction $N(^4S) + CH_2Br$.

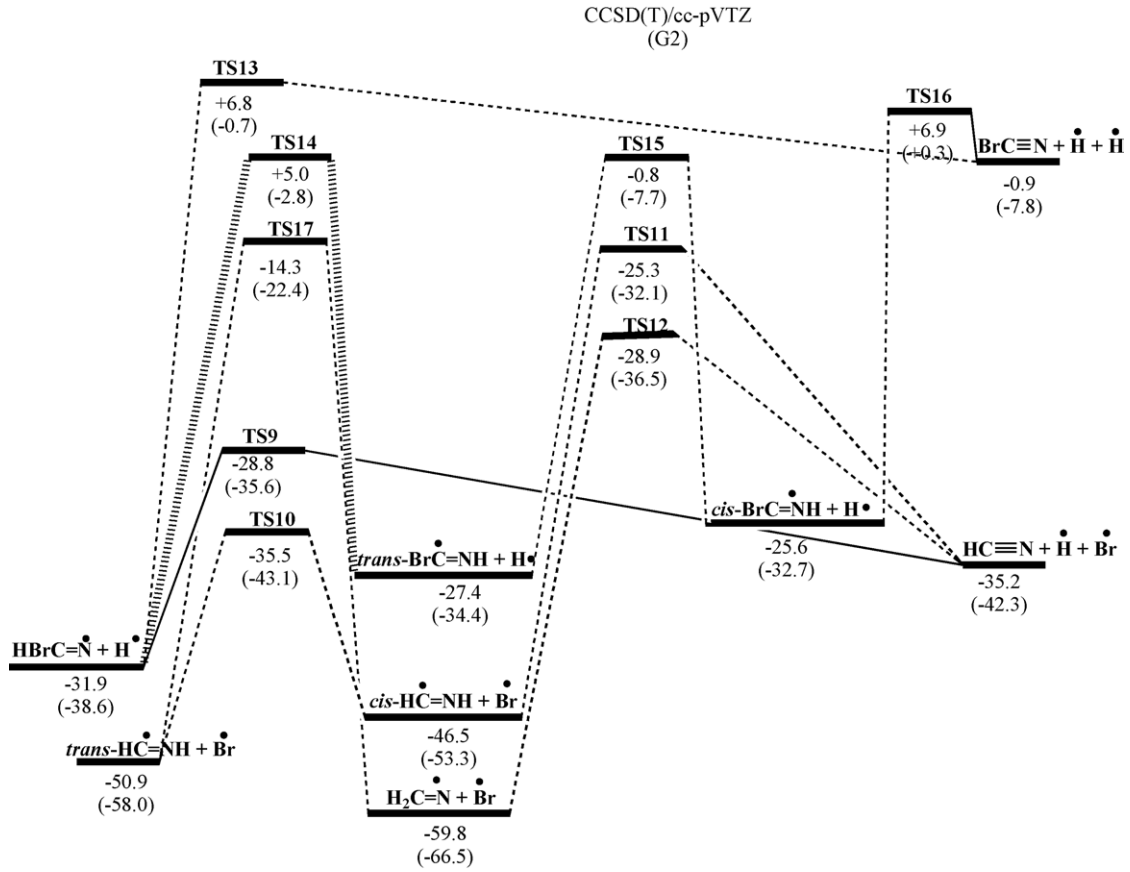

Fig. 5. Reaction profile (kcal mol^{-1}) at the CCSD(T)/cc-pVTZ and G2 (in parentheses) levels for the possible further evolution of the primary products.

tion, the B3LYP $\langle S^2 \rangle$ values are rather close to the spin-pure value in all cases.

Before going on to discuss on the most interesting features of the [NCH_2Br] triplet PES let us comment that, in order to provide information of chemical interest about the electronic structure of the different species shown in Figs. 1 and 2, in the discussion we will represent "limiting structures" taking into account the spin densities of the different atoms. Thus, for example, $H_2C^{\bullet}BrN^{\bullet}$ represents a structure with pronounced diradical character "mainly" ascribed to the carbon and nitrogen atoms.

Approach of N(^{4}S) atoms to $CH_2Cl(^2B_1)$ may take place either through the halogen or carbon atoms. In the first case, MP2 and B3LYP predict two geometrically different intermediates, **I0** (both are $^3A''$; see Fig. 2). At the MP2 level, this species has a Br–N bond distance of 1.815 Å and a spin density at the nitrogen atom of −2. We can thus schematically represent it as $H_2C^{\bullet}BrN^{\bullet}$. At the B3LYP level, **I0** is a weakly bound molecule with a Br–N bond distance of 3.196 Å. The analysis of the atomic spin densities shows that it can be represented as $H_2C^{\bullet}–Br\cdots N^{\bullet\bullet\bullet}$. From the energetic point of view, **I0** is predicted to be either isoenergetic with reactants (ΔH_0 = +0.8 kcal mol^{-1}, at the CCSD(T)/cc-pVTZ//B3LYP/cc-pVTZ level, see Table 1) or clearly endothermic (ΔH_0 = +20.9 kcal mol^{-1}, at the G2 level). In fact, the main reason for the rather different relative energies at the G2 and CCSD(T) levels for **I0** is the very different geometries at both levels (essentially the Br–N distance). We have checked that, at the B3LYP level, forcing the reactants to approach at closer distances than 3.196 Å produces a repulsive surface. We can therefore conclude that approaching of reactants through the bromine atom to form intermediate **I0** is not an exothermic process and will therefore not play a major role in the title reaction in the gas-phase. Finally, we would like to comment that we have also explored the possibility of an intermediate with a $^3A'$ electronic state, but the species we have found are less stable than the $^3A''$ intermediates at both the MP2 and B3LYP levels of theory.

If N(^{4}S) atoms approach $CH_2Cl(^2B_1)$ through the carbon atom the intermediate **I1** ($^3A''$) is formed. This is a direct process which does not involve any transition state. To check that this is in fact the case we have performed scans of the B3LYP and MP2 potential energy surfaces approaching the reactants at different C–N distances and optimizing all other geometrical parameters. They clearly show that reactants interact on an attractive potential surface. Intermediate **I1** lies well bellow the reactants: −63.3 kcal mol^{-1} at the CCSD(T)/cc-pVTZ level (from now on, the CCSD(T) energies will be used unless otherwise stated).

Intermediate **I1** can evolve in three different ways (see Fig. 4): bromine abstraction through **TS1** to yield the most exothermic products of the reaction $H_2C{=}N^{\bullet}$ + Br, hydrogen abstraction through **TS2** to give $HBrC{=}N^{\bullet}$ + H and, finally, hydrogen migration from the carbon to the nitrogen atom (**TS3**) to yield the intermediate $HClC^{\bullet}N^{\bullet}H$, **I2**. Regarding the first process, CCSD(T) predicts **TS1** to lie slightly below the products (of course, at the B3LYP/cc-pVTZ level this transition structure lies above the products) whereas G2 predicts **TS1** to lie only 1.3 kcal mol^{-1} above them. This suggests that release of bromine from **I1** is probably a direct process which requires no more activation energy than its own endothermicity which is actually rather low (ΔH_0 = +3.5 kcal mol^{-1}). Hydrogen abstraction from **I1** through **TS2** requires to overcome a barrier of 36.9 kcal mol^{-1}. This process yields the products $HBrC{=}N^{\bullet}$ + H which are 31.9 kcal mol^{-1} below the reactants. Finally, formation of intermediate **I2** from **I1** through hydrogen migration involves a high barrier of 43.4 kcal mol^{-1}, although **TS3** still lies 19.9 kcal mol^{-1} lower in energy than the reactants.

Once intermediate **I2** is formed new possibilities are opened. First, **I2** can release atomic hydrogen to yield *trans*-$BrC^{\bullet}{=}NH$ + H (ΔH_0 = −27.4 kcal mol^{-1}) and $HBrC{=}N^{\bullet}$ + H (ΔH_0 = 31.9 kcal mol^{-1}). These two processes involve relatively high barriers: 34.2 kcal mol^{-1} (**TS4**) and 26.6 kcal mol^{-1} (**TS5**), respectively. On the other hand, abstraction of bromine from **I2** to give *trans*-$HC^{\bullet}{=}NH$ + Br requires only 5.2 kcal mol^{-1} (**TS6**). The products of this process are the second most exothermic products of the reaction, namely ΔH_0 = −50.9 kcal mol^{-1}. Finally, **I2** may evolve through a new hydrogen migration from carbon to nitrogen to yield the intermediate $BrC^{\bullet\bullet}NH_2$, **I3**. This intermediate is very stable lying 53.7 kcal mol^{-1} below the reactants and only 9.6 kcal mol^{-1} above **I1**. However, formation of **I3** involves the high-lying transition state **TS7** (ΔH_0 = −11.2 kcal mol^{-1}).

Intermediate **I3** may further evolve by both hydrogen and halogen abstraction. The first process yields the products *trans*-$BrC^{\bullet}{=}NH$ + H through a relatively high barrier of 33.5 kcal mol^{-1} (**TS8**). On the other hand, abstraction of a bromine atom is a direct product, since no transition state has been found on the MP2 and B3LYP energy surfaces. This process yields $^{\bullet}CNH_2$ + Br and its endothermicity is 24.3 kcal mol^{-1}.

Once the primary products are formed (see Fig. 4) we can think about the possible evolution of these species by further elimination of either bromine or hydrogen atoms. These processes, which have been summarized in Fig. 5, would lead to the two possible secondary products of the title reaction: BrCN + H + H and HCN + H + Br. As expected, formation of HCN is more favorable from the thermochemical point of view (see Fig. 5 and Table 2), due to the fact that the C–H bond is stronger than the C–Br bond. Production of BrCN (together with elimination of two hydrogen atoms) is little exothermic whereas formation of HCN + H + Br has ΔH_0 = −35.2 kcal mol^{-1}. We remind the reader that these energies are given with respect to the reactants. It must be taken into account, however, that

Table 2
Reaction product branching fractions at different temperatures

T (K)	H_2CN + Br	*t*-HCNH + Br	HBrCN + H
100	0.985	0.001	0.015
150	0.985	0.001	0.015
200	0.984	0.001	0.015
250	0.984	0.001	0.015
300	0.984	0.001	0.016
350	0.983	0.001	0.016
400	0.983	0.001	0.017
450	0.982	0.001	0.017
500	0.982	0.001	0.018

a considerable amount of internal energy should have already been removed by the released bromine and hydrogen atoms during formation of the primary products. We therefore think that the only process leading to a secondary product that can play a relatively important role in this reaction is formation of HCN + H + Br from HBrC=N + H through **TS9**, for it requires to overcome a barrier of only 3.1 kcal mol^{-1}. Moreover, HCN + H + Br lies 3.3 kcal mol^{-1} lower than HBrC=N + H. Other two possible pathways that lead to formation of HCN are, on the one hand, elimination of hydrogen atom from H_2CN and, on the other, isomerization of *trans*-HC=NH to *cis*-HC=NH followed by elimination of a hydrogen atom. The first process should not be feasible because of its endothermicity (ΔH_0 = 24.6 kcal mol^{-1}). Besides, elimination of hydrogen from H_2CN requires to overcome a barrier of 30.9 kcal mol^{-1}. In any case, the feasibility of this process will mainly depend on the amount of internal energy retained by H_2CN. The second process involves isomerization of *trans*-HC=NH into *cis*-HC=NH (which is about 5 kcal mol^{-1} less stable than the trans conformer) followed by hydrogen elimination. The net barrier for this process is 25.9 kcal mol^{-1}. Besides, this process has an endothermicity of 15.7 kcal mol^{-1}.

We would finally like to comment that formation of BrCN from HBrC=N involve transition states that lie quite high in energy (viz. **TS13**, **TS14**, **TS15** and **TS16**). This makes formation of BrCN a highly improbable process in view of our energetic results.

To summarize, we have seen that the most exothermic primary products of the reaction are those in which a bromine atom is released from **I1** and **I2**: $H_2C{=}N^{\bullet}$ + Br and *trans*-$HC^{\bullet}{=}NH$ + Br, respectively. This is due to the large stability of the intermediates and the low strength of the C–Br bond (the endothermicity of these two processes is 3.5 and 1.0 kcal mol, respectively). However, it must be noted that release of a bromine atom from intermediate **I3** ($\Delta H_0 = -53.7$ kcal mol^{-1}) yields one of the less exothermic among the considered products of this reaction: $^{\bullet}CNH_2$ + Br ($\Delta H_0 = -29.4$ kcal mol^{-1}) due to the marginally larger dissociation energy of the C–Br bond in this intermediate. Further evolution of the primary formed species will strongly depend on the amount of energy removed by the released hydrogen and bromine atoms. We consider that the most feasible process leading to a secondary product is elimination of a hydrogen atom from HBrCN, which requires about 3.1 kcal mol^{-1} and has an exothermicity of ca. 3 kcal mol^{-1}.

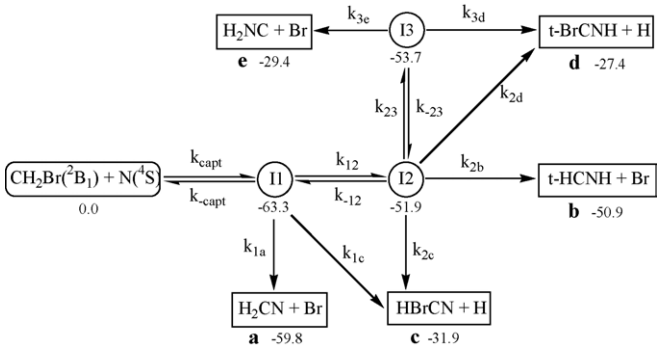

Scheme 1. Mechanistic model for the kinetic study employed in the present work (relative energies at 0 K are in kcal mol^{-1} and were computed at the CCSD(T)/cc-pVTZ level, including B3LYP/cc-pVTZ ZPVEs).

4. Kinetic calculations

The analysis of the PES determined for the triplet [NCH_2Br] system led us to propose a mechanistic model for the reaction of N(^{4}S) with CH_2Br radicals which is schematically depicted in Scheme 1. The proposed mechanistic model includes all the primary products resulting from elimination of either bromine or hydrogen atoms from the different intermediates **I1**, **I2**, and **I3**. The channels are denoted in order of decreasing exothermicity as: a (H_2CN + Br); b (*trans*-HCNH + Br); c (HBrCN + H); d (*trans*-BrCNH + H); e (H_2NC + Br).

The steady-state solution of the master equation leads to the following microcanonical expression for the overall rate coefficient:

$$k_{\text{overall}}(T) = k_{\text{a}}(T) + k_{\text{b}}(T) + k_{\text{c}}(T) + k_{\text{d}}(T) + k_{\text{e}}(T) \tag{3}$$

where the individual coefficients for the different channels are given by the following formulas:

$$k_{\text{a}}(T) = \frac{1}{hQ_{\text{r}}(T)}\sum_J (2J+1)\int_0^{\infty} \frac{N_{\text{capt}}(E,J)k_{1\text{a}}(E,J)}{B(E,J)} \exp\left(-\frac{E}{kT}\right) \mathrm{d}E \tag{4}$$

$$k_{\text{b}}(T) = \frac{1}{hQ_{\text{r}}(T)}\sum_J (2J+1)\int_0^{\infty} \frac{N_{\text{capt}}(E,J)k_{12}(E,J)k_{2\text{b}}(E,J)}{A(E,J)B(E,J)} \exp\left(-\frac{E}{kT}\right) \mathrm{d}E \tag{5}$$

$$k_{\text{c}}(T) = \frac{1}{hQ_{\text{r}}(T)}\sum_J (2J+1)\int_0^{\infty} \frac{N_{\text{capt}}(E,J)}{B(E,J)} \left\{k_{1\text{c}}(E,J) + \frac{k_{12}(E,J)k_{2\text{c}}(E,J)}{A(E,J)}\right\} \exp\left(-\frac{E}{kT}\right) \mathrm{d}E \tag{6}$$

$$k_{\text{d}}(T) = \frac{1}{hQ_{\text{r}}(T)}\sum_J (2J+1)\int_0^{\infty} \frac{N_{\text{capt}}(E,J)k_{12}(E,J)}{A(E,J)B(E,J)} \left\{k_{2\text{d}}(E,J) + \frac{k_{23}(E,J)k_{3\text{d}}(E,J)}{k_{-23}(E,J)+k_{3\text{d}}(E,J)+k_{3\text{e}}(E,J)}\right\} \exp\left(-\frac{E}{kT}\right) \mathrm{d}E \tag{7}$$

$$k_{\text{c}}(T) = \frac{1}{hQ_{\text{r}}(T)}\sum_J (2J+1)\int_0^{\infty} \frac{N_{\text{capt}}(E,J)k_{12}(E,J)k_{23}(E,J)k_{3\text{e}}(E,J)}{A(E,J)B(E,J)[k_{-23}(E,J)+k_{3\text{d}}(E,J)+k_{3\text{e}}(E,J)]} \exp\left(-\frac{E}{kT}\right) \mathrm{d}E \tag{8}$$

where $N_{capt}(E, J)$ is the number of the states evaluated in the barrier-free process as described in the methodological section, $Q_r(T)$ are the reactants relative translational partition function at the temperature T and $A(E, J)$ and $B(E, J)$ were calculated according to the following relations.

$$A(E, J) = k_{-12}(E, J) + k_{23}(E, J) + k_{2b}(E, J) + k_{2c}(E, J) + k_{2d}(E, J) - \frac{k_{23}(E, J)k_{-23}(E, J)}{k_{-23}(E, J) + k_{3d}(E, J) + k_{3e}(E, J)} \quad (9)$$

$$B(E, J) = k_{-capt}(E, J) + k_{12}(E, J) + k_{1a}(E, J) + k_{1c}(E, J) - \frac{k_{12}(E, J)k_{-12}(E, J)}{A(E, J)} \quad (10)$$

The overall and individual canonical rate coefficients are represented in Fig. 6 as functions of the temperature. Both channels d (production of *trans*-BrCNH + H) and e (formation of $H_2NC + Br$) have rate coefficients that are much smaller than the other ones and therefore they are not shown in Fig. 6. The estimated activation free energy for the overall process is just 0.09 kcal mol^{-1}. This value is consistent with a barrier-free process as evidenced by the analysis of the PES. The computed rate coefficient for the overall process at 300 K is 9×10^{-13} cm^3 s^{-1} molecule^{-1}, a value somewhat smaller than the corresponding estimated value for the reaction of nitrogen atoms with fluoromethyl radicals[15]

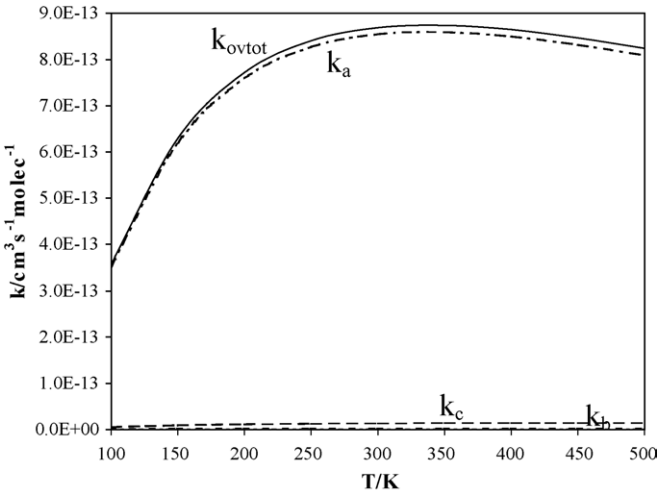

Fig. 6. Overall and individual canonical rate coefficients (cm^{-3} s^{-1} molecule^{-1}) plotted vs. temperature.

(13 × 10^{-13} cm^3 s^{-1} molecule^{-1}) but nearly three times larger than the rate coefficient for the N(^{4}S) + CH_2Cl reaction [16] (3 × 10^{-13} cm^3 s^{-1} molecule^{-1}). Nevertheless, we must point out that these values should only be considered valid at a semi-quantitative level, given the approximations made in the application of RRKM theory to the processes under study and also in the light of our recent results based on molecular dynamics simulations [16]. It is clear that the three reactions with nitrogen

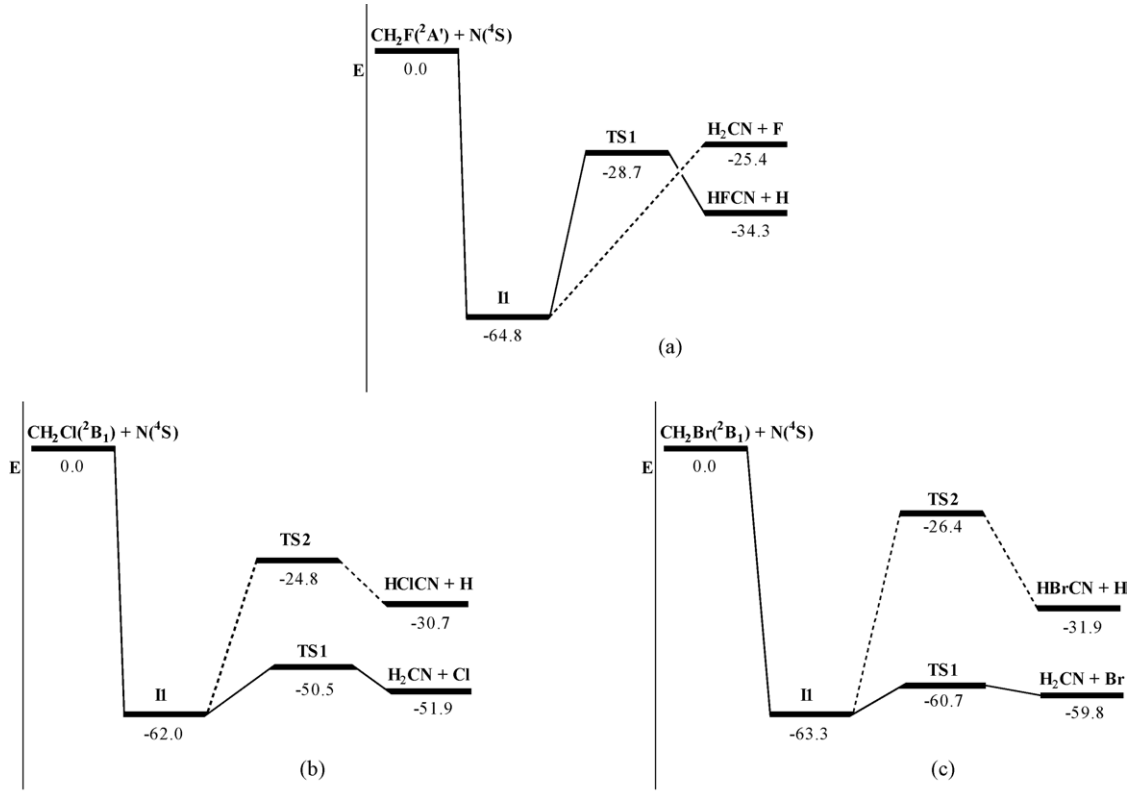

Fig. 7. Schematic representation of the two most competitive channels for the reaction N(^{4}S) + CH_2F (panel a), N(^{4}S) + CH_2Cl (panel b), and N(^{4}S) + CH_2Br (panel c). Relative energies (kcal mol^{-1}) have been obtained at the CCSD(T)/cc-pVTZ level including B3LYP/cc-pVTZ ZPE.

atoms (CH_2F, CH_2Cl, and CH_2Br) are rather efficient processes proceeding at near collision-efficiency.

The individual rate coefficients for the present reaction follow the same trends than in the case of the $N(^4S) + CH_2Cl$ reaction [16]. From inspection of Fig. 6 it is clear that channel a is the dominant one, followed at a large distance by channel c. A qualitative ordering of the individual rate coefficients according to their magnitudes, produces the following result: $k_a \gg k_c > k_b \gg k_d \approx k_e$. The corresponding product branching ratios (only for those channels with significant values) at different temperatures are collected in Table 2. It is clearly seen that the dominant channel (with branching fractions always above 0.98) for the reaction of nitrogen atoms with bromomethyl radicals is the most exothermic channel, namely channel a leading to $H_2CN + Br$. The results shown in Table 2 also show that the most important secondary channel (under kinetic control) should be channel c, leading to HBrCN + H, although only in residual quantities. It should be noticed that production of HBrCN + H is less endothermic than production of *t*-HCNH+Br.

The kinetic results are consistent with the general overview of the PES for the triplet $[NCH_2Br]$ system shown in Fig. 4. All channels start from the formation of intermediate **I1**, which does not imply any energy barrier. From this intermediate there are two direct processes leading respectively to $H_2CN + Br$ (through **TS1**) and HBrCN + H (involving **TS2**). The former should be clearly favored, because it implies a barrier (relative to **I1**) of just 2.6 kcal mol^{-1}, whereas **TS2** lies about 36.9 kcal mol^{-1} above **I1**. Channel b, which leads to *t*-HCNH + Br, necessarily involves isomerization of **I1** into **I2**. The associted transition state, **TS3**, lies even higher in energy (about 43.4 kcal mol^{-1} above **I1**), and therefore channel b is even less competitive than channel c.

We may now compare the most relevant mecahnistic aspects for the reactions of nitrogen atoms with the different halomethyl radicals. In Fig. 7 we have schematically represented the two most competitive channels for the reactions of $N(^4S)$ with CH_2F, CH_2Cl, and CH_2Br. It is readily seen in Fig. 7 that for the reactions with CH_2Cl and CH_2Br the overall picture is quite similar. The magnitude of the reaction enthalpies and energy barriers are even quite close. The preferred product, both from thermodynamic and kinetic points of view, is $H_2CN + X$. In fact, there is a large difference in the relative energies of transition states **TS1** and **TS2** for both chloromethyl and bromomethyl radicals. As a consequence, not only the $H_2CN + X$ channel is favored, but it is clearly predominant over HXCN + H. On the other hand, in the case of the fluorinated radical, the HXCN + H channel is favored both thermodynamically and kinetically. However, the $H_2CN + F$ channel involves an energy barrier only slightly higher than the HFCN + H channel. The result is that $H_2CN + F$ should be the dominant channel, but with HFCN + H having a significant contribution.

5. Conclusions

A theoretical study of the reaction of $N(^4S)$ with CH_2Br radicals has been carried out on the triplet surface. The reaction starts by approaching the nitrogen atom to carbon, which results in the formation of a relatively stable intermediate (63.3 kcal mol^{-1} below reactants at the CCSD(T)/cc-pVTZ level). This is a direct process which does not involve any energy barrier. Elimination of bromine from this intermediate leads to the most exothermic products, $H_2C{=}N + Br$ (−59.8 kcal mol^{-1}). Elimination of a hydrogen atom produces less exothermic products, HBrCN + H (−31.9 kcal mol^{-1}). The channel proceeding through isomerization of the initial intermediate, followed by elimination of bromine to form *trans*-HC=NH + Br (−50.9 kcal mol^{-1}), is even more exothermic than HBrCN + H.

A kinetic study, within the framework of the statistical theories, of the $N(^4S) + CH_2Br$ reaction confirms that the most exothermic product, namely $H_2C{=}N + Br$, is also the preferred product under kinetic control. The estimated branching ratio for $H_2C{=}N + Br$ is about 0.98, and only minor fractions of HBrCN + H are predicted at all temperatures. Therefore, the behavior observed for the $N(^4S) + CH_2Br$ reaction is very similar to its analogue starting from chloromethyl radicals. In both cases, the predicted dominant channel corresponds to formation of H_2CN through elimination of the halogen atom. On the other hand, for the reaction of ground-state nitrogen atoms with CH_2F the preferred channel, both from the thermodynamic and kinetic points of view, involves the elimination of a hydrogen atom and formation of a product containing a carbon–halogen bond, namely HFCN. The common characteristic for the three reactions of $N(^4S)$ with halomethyl radicals is that the all of them are predicted to proceed with a rather high efficiency.

Acknowledgement

This research has been supported by the Ministerio de Educación y Ciencia of Spain (Grants CTQ2004-07405 and HI2002-0025) and by the Junta de Castilla y León (Grant VA085/03). AC gratefully acknowledges a fellowship from the Junta de Castilla y León.

Appendix A. Supplementary data

Supplementary data associated with this article can be found, in the online version, at 10.1016/j.ijms.2005.11.008.

References

[1] J.A. Seetula, I.R. Slagle, D. Gutman, S.M. Senkan, Chem. Phys. Lett. 252 (1996) 299.
[2] J.A. Seetula, I.R. Slagle, Chem. Phys. Lett. 277 (1997) 381.
[3] Y. Yamamori, K. Takahashi, T. Inomata, J. Phys. Chem. A 103 (1999) 8803.
[4] S.I. Stoliarov, A. Bencsura, E. Shafir, V.D. Knyazev, I.R. Slagle, J. Phys. Chem. A 105 (2001) 76.
[5] C. Tsai, S.M. Belanger, J.T. Kim, J.R. Lord, D.L. McFadden, J. Phys. Chem. 93 (1989) 1916.
[6] C. Tsai, D.L. McFadden, J. Phys. Chem. 94 (1990) 3298.
[7] S.C. Jeoung, K.Y. Choo, S.W. Benson, J. Phys. Chem. 95 (1991) 7282.
[8] S.V.K. Kumar, N. Sathyamurthy, S. Manogaran, S.K. Mitra, Chem. Phys. Lett. 222 (1994) 465.
[9] B. Wang, H. Hou, Y. Gu, J. Phys. Chem. A 103 (1999) 2060.
[10] B. Wang, H. Hou, Y. Gu, J. Phys. Chem. A 103 (1999) 5075.
[11] H. Hou, B. Wang, Y. Gu, J. Phys. Chem. A 103 (1999) 8075.
[12] B. Wang, H. Hou, Y. Gu, Chem. Phys. Lett. 304 (1999) 278.
[13] B. Wang, H. Hou, Y. Gu, Chem. Phys. 247 (1999) 201.

[14] B. Menendez, V.M. Rayon, J.A. Sordo, A. Cimas, C. Barrientos, A. Largo, J. Phys. Chem. A 105 (2001) 9917.
[15] A. Cimas, M. Aschi, C. Barrientos, V.M. Rayon, J.A. Sordo, A. Largo, Chem. Phys. Lett. 374 (2003) 594.
[16] A. Cimas, V.M. Rayon, M. Aschi, C. Barrientos, J.A. Sordo, A. Largo, J. Chem. Phys. 123 (2005) 114312.
[17] R.P. Wayne, Chemistry of Atmospheres, Oxford University Press, Oxford, 1991.
[18] B. Finlayson-Pitts, J.N. Pitts, Chemistry of the Upper and Lower Atmosphere, Academic Press, San Diego, 1999.
[19] G. Marston, F.L. Nesbitt, D.F. Nava, W.A. Payne, L.J. Stief, J. Phys. Chem. 93 (1989) 5769.
[20] G. Marston, F.L. Nesbitt, L.J. Stief, J. Chem. Phys. 91 (1989) 3483.
[21] C. Gonzalez, H.B. Schlegel, J. Am. Chem. Soc. 114 (1992) 9118.
[22] R.G. Sadygov, D.R. Yarkony, J. Chem. Phys. 107 (1997) 4994.
[23] L.A.M. Nejad, T.J. Millar, Mon. Not. R. Astron. Soc. 230 (1988) 79.
[24] Y.L. Yung, M. Allen, J.P. Pinto, Astrophys. J. Suppl. Ser. Phys. 55 (1984) 465.
[25] P. Glarborg, J.A. Miller, R.J. Kee, Combust. Flame 65 (1986) 177.
[26] W.J. Hehre, L. Radom, P.V.R. Schleyer, J.A. Pople, Ab initio Molecular Orbital Theory, Wiley, NY, 1986.
[27] W. Koch, M.C. Holthausen, A Chemist's Guide to Density Functional Theory, 2nd ed., Wiley–VCH, Weinheim, 2000.
[28] T.H. Dunning Jr., J. Chem. Phys. 90 (1989) 1007.
[29] A.D. Becke, J. Chem. Phys. 97 (1992) 9173.
[30] C. Lee, W. Yang, R.G. Parr, Phys. Rev. B 37 (1988) 785.
[31] T.H. Dunning Jr., J. Phys. Chem. A 104 (2000) 9062.
[32] D. Feller, J.A. Sordo, J. Chem. Phys. 113 (2000) 485.
[33] H.B. Schlegel, J. Chem. Phys. 84 (1986) 4530.
[34] R.J. Bartlett, J.F. Bartlett, Stanton Reviews in Computational Chemistry, vol. 5, VCH, New York, 1994.
[35] L.A. Curtiss, K. Raghavachari, G.W. Trucks, J.A. Pople, J. Chem. Phys. 94 (1991) 7221.
[36] C. Gonzalez, H.B. Schlegel, J. Chem. Phys. 90 (1989) 2154.
[37] C. Gonzalez, H.B. Schlegel, J. Chem. Phys. 94 (1990) 5523.
[38] M.J. Frisch, G.W. Trucks, H.B. Schlegel, G.E. Scuseria, M.A. Robb, J.R. Cheeseman, V.G. Zakrzewski, J.A. Montgomery Jr., R.E. Stratmann, J.C. Burant, S. Dapprich, J.M. Millan, A.D. Daniels, K.N. Kudin, M.C. Strain, O. Farkas, J. Tomasi, V. Barone, M. Cossi, R. Cammi, B. Mennucci, C. Pomelly, C. Adamo, S. Clifford, J. Ochterski, G.A. Petersson, P.Y. Ayala, Q. Cui, K. Morokuma, D.K. Malick, A.D. Rabuck, K. Raghavachari, J.B. Foresman, J. Cioslowski, J.V. Ortiz, A.G. Baboul, B.B. Stefanov, G. Liu, A. Liashenko, P. Piskorz, I. Komaromi, R. Gomperts, R.L. Martin, D.J. Fox, T. Keith, M.A. Al-Laham, C.Y. Peng, A. Nanayakkara, C. Gonzalez, M. Challacombe, P.M.W. Gill, B. Johnson, W. Chen, M.W. Wong, J.L. Andres, M. Head-Gordon, E.S. Replogle, J.A. Pople, Gaussian 98, Gaussian Inc., Pittsburg, PA, 1998.
[39] B.C. Garrett, D.G. Truhlar, J. Chem. Phys. 70 (1979) 1593.
[40] X. Hu, W.L. Hase, J. Chem. Phys. 95 (1991) 8073.
[41] W.H. Miller, N.C. Handy, J.E. Adams, J. Chem. Phys. 72 (1980) 99.
[42] A.G. Baboul, H.B. Schlegel, J. Chem. Phys. 90 (1989) 2154.
[43] P.J. Robinson, K.A. Holbrook, Unimolecular Reactions, Wiley, New York, 1972.
[44] W. Forst, Theory of Unimolecular Reactions, Academic, New York, 1973.
[45] W.H. Miller, J. Am. Chem. Soc. 101 (1979) 6810.
[46] S. Bailleux, P. Drèan, M. Godon, Z. Zelinger, C. Duan, Phys. Chem. Chem. Phys. 6 (2004) 3049.
[47] S. Bailleux, P. Drèan, Z. Zelinger, S. Civiš, H. Ozeki, S. Saito, J. Chem. Phys. 122 (2005) 134302.
[48] B.J. Lynch, D.G. Truhlar, J. Phys. Chem. A 105 (2001) 2936.
[49] T.J. Lee, P.R. Taylor, Int. J. Quantum Chem. Symp. 23 (1989) 199.